Journal of Nuclear Materials 415 (2011) S1098–S1101

Contents lists available at ScienceDirect

Journal of Nuclear Materials

journal homepage: www.elsevier.com/locate/jnucmat

3-D reconstruction of pre-characterized lithium and tungsten dust particle trajectories in NSTX

J. Nichols [a,*], A.L. Roquemore [b], W. Davis [b], D.K. Mansfield [b,1], C.H. Skinner [b], E. Feibush [b], W. Boeglin [c], R. Patel [c], D. Abolafia [d], K. Hartzfeld [e], R. Maqueda [f]

[a] Cornell University, Ithaca, NY 14853, USA
[b] Princeton Plasma Physics Laboratory, Princeton, NJ 08543, USA
[c] Florida International University, Miami, FL 33199, USA
[d] The Bergen County Academies, Hackensack, NJ 07601, USA
[e] Toms River High School, Toms River, NJ 08753, USA
[f] Nova Photonics, Inc., Princeton, NJ 08540, USA

ARTICLE INFO

Article history:
Available online 2 November 2010

ABSTRACT

Calibrated amounts of 40 μm lithium dust and 10 μm tungsten powder have been dropped from above into the SOL of the National Spherical Torus Experiment (NSTX) to benchmark modeling of dust dynamics and transport. By combining the output from two visible-range fast cameras, 3-D trajectories are reliably obtained and have resulted in the generation of several hundred individual particle tracks. Particles are observed to undergo a variety of accelerations both parallel and perpendicular to the magnetic field, as well as abrupt large-angle changes in direction. All tracks obtained to date display particle motion that is constrained to within a few centimeters of the last closed flux surface. The 3-D trajectories are presented and compared to the location of the last closed flux surface as determined by EFIT.

1. Introduction

Microscopic dust particles are routinely observed during operation of magnetic confinement fusion devices around the world. This dust has not had a major effect on the operation of modern fusion devices, but due to the increased operational time and vastly higher power and particle fluxes of next-generation machines such as ITER, in-vessel dust inventories are expected to increase by orders of magnitude and potentially approach key safety and stability limits [1]. Excessive dust inventories could lead to radiological concerns and explosion hazards, as well as hinder diagnostics and degrade plasma performance [2]. In order to combat and control dust buildup in ITER, it is necessary to understand the dynamics of dust in a fusion-grade plasma. To this end, the Dust Transport (DUSTT) code developed at UCSD has been coupled to the edge plasma transport code UEDGE to model dust motion in tokamaks and spherical tori and the first comparison results between theory and experiment have been obtained using the data presented in this paper [3].

This study focuses on obtaining the experimental data required to validate the DUSTT code. Lithium particles were introduced into the National Spherical Torus Experiment (NSTX) at PPPL using recently developed piezo crystal-based powder droppers and their trajectories were observed with fast cameras [4]. The lithium particles are passivated spheres with diameters between 40 and 44 μm (measured by the manufacturer), encased in a 40 nm thick shell of carbon. While lithium is not presently planned for use inside of the ITER vessel, it is very close in mass to beryllium (a key ITER first-wall material) and is expected to have very similar dynamics, while being much safer to handle. During a discharge, the lithium dust is invisible until it enters the plasma, where the ablated material surrounding each particle is excited by electron bombardment and emits visible light (as discussed in Section 3) that can be captured by visible-range fast cameras [5].

Tungsten dust is a first-wall material in the ITER divertor, so its behavior is especially important to characterize. We were able to obtain one discharge with tungsten injection on the next to the last shot of the 2009 campaign. At that time the toroidal field direction was reversed compared to that used for the Li experiments, making it difficult to make a direct comparison between lithium and tungsten trajectories. Still, some interesting results were obtained and are described in Section 4. The tungsten particles were of odd shapes with maximum dimension of 10 μm.

2. Camera setup, tracking, and reconstruction

For rigorous three dimensional (3-D) dust tracking, it is imperative that two cameras be used. A similar camera setup was used as

* Corresponding author. Address: Princeton Plasma Physics Laboratory, POB 451, Princeton, NJ 08543, USA.
E-mail addresses: jnichols@pppl.gov (J. Nichols), dmansfie@pppl.gov (D.K. Mansfield).
[1] Presenting author.

0022-3115/$ - see front matter © 2010 Elsevier B.V. All rights reserved.
doi:10.1016/j.jnucmat.2010.10.049

in previous experiments [6] with one wide-view fast camera (a Phantom 7.3 manufactured by Vision Research) placed at Bay L and one narrow-view fast camera (a Phantom 4.2, also by Vision Research) at Bay B, as seen in Fig. 1. Natural dust (from the divertor, RF antennas, etc.) is rarely observed in this region, so we assume that all observed particles originated at the dropper. The cameras were operated at 7000–10,000 frames per second at resolutions ranging from 224 × 200 pixels to 320 × 240 pixels. The primary tool for determining the dust location was the IDL application "fcplayer," developed at PPPL [7]. In cases when the particles were difficult to locate, background subtraction, gamma correction, and threshholding were utilized to aid the process. The two sets of 2D pixel positions were then transformed into 3-D trajectories using a set of Python modules developed at Florida International University, which have been previously described in Ref. [8]. Smoothing was applied to the trajectories in order to eliminate the rapid oscillations that arise from limited pixel resolution.

3. Lithium particle results

A total of 215 lithium particle trajectories were generated from eight NSTX discharges (shots 130376–9, 130388–9, 135352–3). Trajectories were measured primarily during plasma current flattop of 0.9 MA. These discharges were heated by NBI, and dust trajectories have been obtained for P_{NBI} of 2, 4, and 6 MW. Once the walls of NSTX have been well-conditioned by extensive operation, it is uncommon to see intrinsic dust particles appear in the midplane views, especially during the current flattop, unless a disruption occurs which typically terminates the discharge. A very high probability therefore exists that the trajectories presented in the data were obtained from particles introduced by the dust dropper.

From observation of hundreds of trajectories, clear patterns regarding the general motion of the particles emerge. We divide the trajectories into two categories according to the primary direction of motion. In the first category particles move from the upper right to lower left (Fig. 2), a direction that has a large component perpendicular to the magnetic field lines and has toroidal motion in the same direction as the plasma current. The curved black lines behind the data points in the figure represent the vessel wall. Depending on machine parameters, the magnetic field pitch at the edge is between 30° and 45° from the horizontal, with a top-left to bottom-right orientation. Difficulties in tracking closely grouped particles make it impossible to use the dust track reconstruction code to generate a sample that is statistically representative of all the particles in the vessel, but it is clear from bulk drift patterns that the vast majority (>90%) of dust particles fall into category I. Since these are the most common, they are of the most interest for predictive purposes. Motion of particles in this category tends to be characterized by slow drifts at near-constant speeds in the range of 10–40 m/s rather than fast streaks and accelerations.

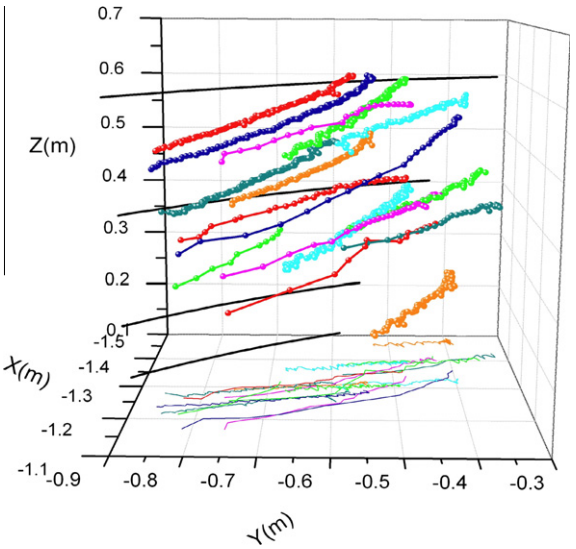

Fig. 2. Category I lithium particle trajectories. More than 90% of the dust particles will fit into this category where particles move from upper right to lower left across the magnetic field lines. Typical velocities of 10–40 m/s are observed.

Category II encompasses the particles moving from the upper left to the lower right or from the lower right to upper left (Fig. 3), and provides a stark contrast to category I. These particles move parallel (or antiparallel) to the magnetic field lines, and are in general much less numerous than their category I counterparts. In addition, most of the particles in this category undergo rapid linear accelerations and reach high speeds of up to 100 m/s, though the occasional slow drift remains.

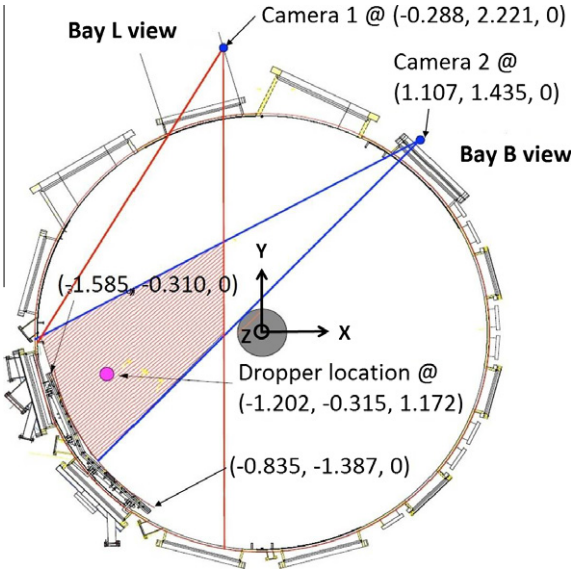

Fig. 1. Camera positions on NSTX midplane along with an indication of their overlapping fields of view. (X, Y, Z) coordinates of important features are marked, with the coordinate system centered at the midplane of the center stack.

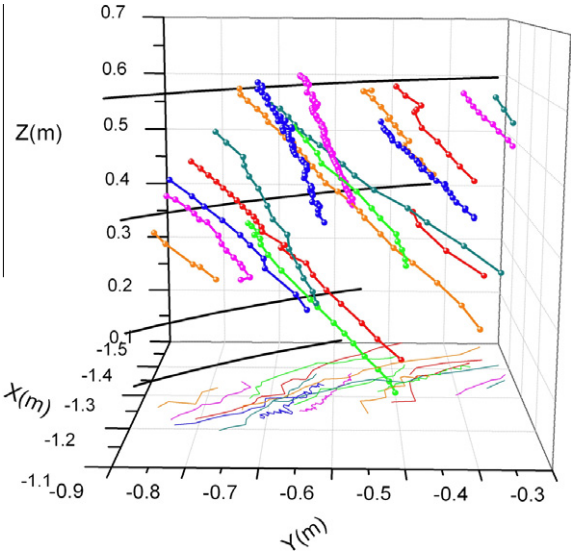

Fig. 3. Category II lithium particle trajectories comprise a much smaller population of particles, with trajectories along the magnetic field line and velocities of up to 100 m/s.

Finally, there are some trajectories that don't fit into either category I or II (Fig. 4). A wide variety of accelerations and direction changes can be seen in these trajectories. There is a general pattern of transitions between category I and category II or vice versa, but some particles make the transition with a quick turn while some follow a leisurely arc. Compared to the thousands of other dust particles in the vessel these oddities are numerically insignificant; however, a scientific explanation for these trajectories is lacking.

If a random sampling of particles from the collected dataset is plotted on one graph and viewed tangentially instead of head-on, it is seen that all of the particles are lined up parallel to the vessel wall. Furthermore, all particles appear to be confined to the narrow region between the wall and the plasma separatrix (as determined by the plasma reconstruction tool EFIT). A 3-D plot of the vessel wall and a few particle tracks is given in Fig. 5. No Li particles are observed to cross the separatrix and enter the main plasma volume. Charge Exchange Recombination Spectroscopy (CHERS) measurements also indicate that Li concentration in the core did not increase during any of the discharges with dust injection (maximum Li dropped: 250 mg) [9].

To further investigate the ionization states of the Li ablated from the dust particles, Li filters were placed in front of the cameras. Fig. 6 shows typical images obtained with Li I and Li II filters. Using the neutral Li I (670.8 nm) filter, the individual particles are clearly observed along with filaments associated with events such as edge localized modes (ELMs). Using the same camera on a near identical discharge with a singly-ionized Li II (548.5 nm) filter, the individual particles are no longer visible, and the frames are mostly dark except during events such as ELMs, where the filaments are very bright. This indicates that the ablation clouds immediately surrounding Li particles are made primarily of excited neutrals, while Li spread more widely around the machine is primarily ionized. This is also evident on the global true-color "Plasma TV," as green Li II light appears throughout the vessel while orange Li I light is limited to the area directly under the powder dropper.

4. Tungsten particle results

During the last two weeks of the 2009 campaign, NSTX operated in a reversed toroidal field configuration. The last three discharges of this campaign (136158-60) were dedicated to tungsten dust, and one discharge had tungsten injection. A number of good trajectories were obtained and were analyzed by the trajectory reconstruction code. Due to the reversed fields, a direct comparison with the Li trajectories taken earlier was not possible. In discharge 136159, the tungsten dust was released at a rate of 3 mg/s throughout the discharge from the same location as the Li dropper. Particles can be seen dropping straight down at the beginning of the discharge, and enter the SOL at a velocity of approximately 5 m/s. The particles then slow considerably as they interact with the plasma and begin to change directions. All observed particles had speeds between 0.5 and 1.7 m/s, with most tending toward the lower end of this range. As the discharge develops and the current flat top is reached, the tungsten particles travel toroidally in the direction of the plasma current similar to the Li particles; however, due to the reversed field configuration, the tungsten particles have developed a clear upward motion to their trajectories (as seen in Fig. 7), so that the particles have a large cross-field velocity component. Injecting the particles into the reversed field configuration was not anticipated in the beginning of the campaign. The particles traversed a region without reliable background position measurements, so calibration of the camera view was performed using design drawings of the tile grid. An error analysis shows this may introduce uncertainties of order 1–6 cm. It is still clear that the tungsten particles move closer to the separatrix than the Li parti-

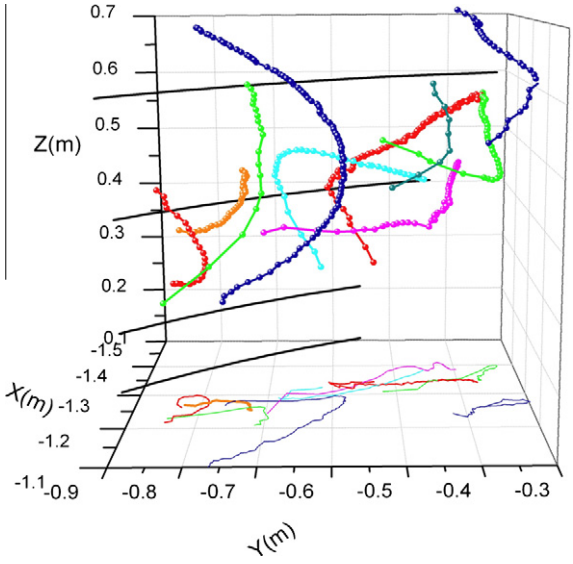

Fig. 4. Particles can undergo abrupt transitions from category I to category II displaying sharp turns in direction. This group comprises less than 1% of the total dust population.

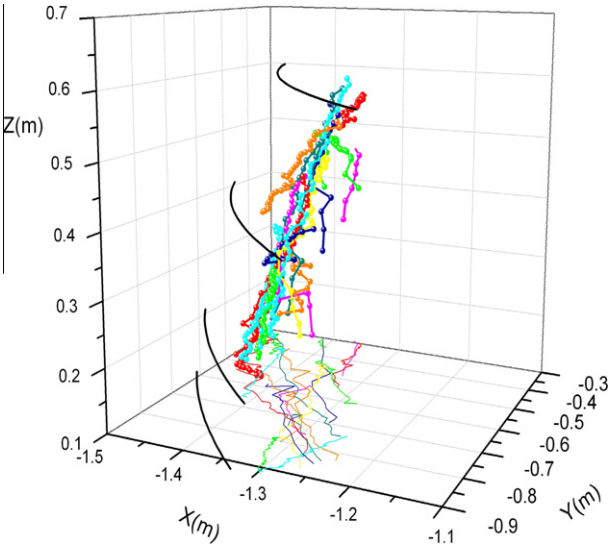

Fig. 5. Random selections of particles from all three Li categories show the particle trajectories are aligned between the separatrix and the vessel wall but do not cross the separatrix.

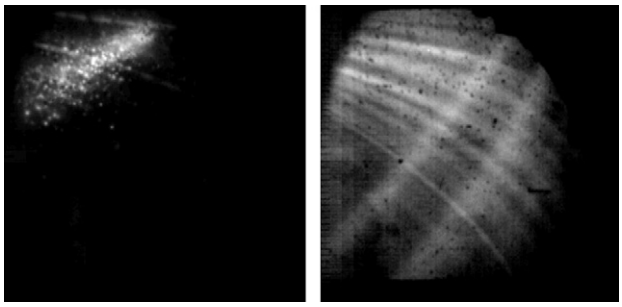

Fig. 6. The left panel shows Li I (670.8 nm) neutral emission, and individual particles can be clearly distinguished. The right panel was taken with a Li II filter (548.5 nm), and shows only filaments illuminated during an ELM. Particles are not distinguishable, indicating no ionization.

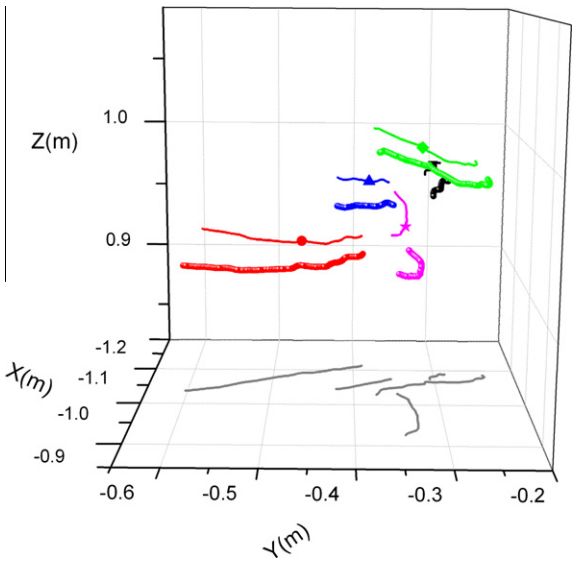

Fig. 7. Tungsten trajectories taken during a reversed field experiment exhibit a slight upward drift (see projections on the Y–Z plane) for the majority of particles.

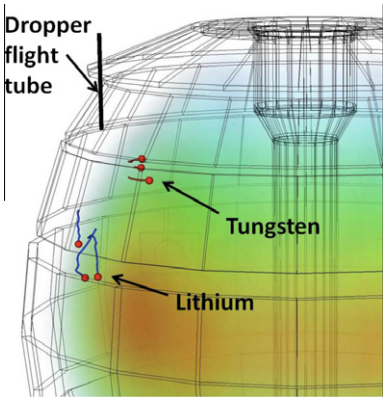

Fig. 8. Indirect comparison between tungsten (red) and Li (blue) trajectories overlaid on a typical NSTX plasma. The tungsten particles are slower, located more inboard and remain elevated higher in the Z-direction. (For interpretation of the references to color in this figure legend, the reader is referred to the web version of this article.)

cles and some of them appear to have penetrated the boundary. This may be due to the smaller dimensions of the tungsten particles making them less affected by the plasma flow. A confirmation of tungsten locations relative to the separatrix may have to wait until careful measurements of the vessel walls can be made during the next vessel opening. Spectroscopic data from the Long Wavelength Extreme Ultraviolet Spectrometer (LoWEUS) did show that silver-like W^{27+} ions made their way into the core of NSTX [10]. Also, the midplane tangential bolometer measured a radiated power profile that was strongly peaked after 500 ms, indicating the presence of high-Z impurities [11]. However, during the subsequent discharge without tungsten injection, there was no spectroscopic evidence of tungsten residue.

5. Discussion

Pre-characterized Li and tungsten dust has been dropped from above into NSTX plasmas to study dust behavior in the SOL. Though a direct comparison between tungsten and Li is not possible because of the different field configurations, it is clear that the tungsten travels at a much smaller velocity than larger Li particles and that the tungsten penetrates deeper into the SOL and appears to just cross the separatrix. No Li particles have yet been observed to cross the separatrix. This may be due to the much larger cross-section that lithium particles present to the plasma ($\sim$16$\times$ greater area despite only $\sim$2$\times$ greater mass) making them more sensitive to the parallel plasma flows in the SOL. The issue of volume and density are explicitly handled by the DUSTT-UEDGE codes. Both species have a toroidal component in the direction of the plasma current but the Li particles had a downward acceleration while the tungsten exhibits a slight upward motion due to the reversed toroidal field. By comparing Figs. 2 and 7 it can be seen that tungsten emission is apparent from $Z = 90$ cm to $Z = 100$ cm while the Li particles are visible $Z = 0$ to $Z = 60$ cm. Fig. 8 is a 3-D visualization of representative tungsten and Li trajectories, where the plasmas had similar parameters but reversed toroidal fields. A more comprehensive investigation into the specific differences in Li and W transport by comparing the respective DUSTT-UDGE models is planned, as well as additional tungsten dust experiments.

Acknowledgements

This work was supported by US DOE Contract #DE-AC02-09CH11466 and the Office of Science's Science Undergraduate Laboratory Internship Program.

References

[1] D.L. Rudakov et al., Rev. Sci. Instrum. 79 (2008) 10F303.
[2] A.Yu. Pigarov et al., Dust Transport in Tokamaks, Sherwood Fusion Theory Conference, Annapolis, MD, 23–25 April 2007.
[3] R.D. Smirnov et al., J. Nucl. Mater., these proceedings.
[4] D.K. Mansfield et al., 2nd NIFS-CRC International Symposium on Plasma-Surface Interactions: NIFS, Toki, Gifu, Japan.
[5] Y. Tanaka et al., Phys. Plasma 14 (2007) 052504.
[6] A.L. Roquemore et al., J. Nucl. Mater. 363–365 (2007) 222–226.
[7] W.M. Davis et al., Fusion. Eng. Des. 85 (2010) 325–327.
[8] W.U. Boeglin et al., Rev. Sci. Instrum. 79 (2008) 10F334.
[9] R.E. Bell, private communication, 2009–2010.
[10] J. Clementson et al., Rev. Sci. Instrum. 81 (2010) 10E326.
[11] S.F. Paul, private communication, 2009.